Competition of Charge-Density Waves and Superconductivity in Sulfur

O. Degtyareva,[1] M. V. Magnitskaya,[2] J. Kohanoff,[3] G. Profeta,[4] S. Scandolo,[5] M. Hanfland,[6] M. I. McMahon,[1] and E. Gregoryanz[1]

[1]*SUPA, School of Physics and Centre for Science at Extreme Conditions, The University of Edinburgh, Edinburgh EH9 3JZ, United Kingdom*

[2]*Institute for High Pressure Physics, Russian Academy of Sciences, Troitsk, Moscow Region 142190, Russia*

[3]*Atomistic Simulation Centre, Queen's University Belfast, Belfast BT7 1NN, Northern Ireland, United Kingdom*

[4]*CNISM-Dipartimento di Fisica, Università degli Studi di L'Aquila, I-67010 Coppito (L'Aquila) Italy*

[5]*The Abdus Salam International Centre for Theoretical Physics (ICTP), Trieste, Italy, and INFM/CNR "Democritos" National Simulation Center, Trieste, Italy*

[6]*ESRF, Boîte Postale 220, 38043 Grenoble, France*

(Received 12 January 2007; published 12 October 2007)

A one-dimensional charge-density wave (CDW) instability is shown to be responsible for the formation of the incommensurate modulation of the atomic lattice in the high-pressure phase of sulfur. The coexistence of, and competition between, the CDW and the superconducting state leads to the previously observed increase of T_c up to 17 K, which we attribute to the suppression of the CDW instability, the same phenomenology found in doped layered dichalcogenides.

DOI: 10.1103/PhysRevLett.99.155505 PACS numbers: 61.50.Ks, 62.50.+p, 74.25.Kc, 74.25.Jb

Various examples of the appearance of the charge-density wave (CDW) state, and its coexistence with the superconducting ground state, are known from experimental and theoretical studies of compounds, such as transition-metal chalcogenides, blue bronzes, charge-transfer salts, and other complex materials [1–3]. Despite the fact that the conceptual possibility of CDW states was suggested many years ago for simple metals [4], uranium has long remained a unique example among the elements forming a CDW [5,6]. However, the application of pressure offers an opportunity to observe a CDW in other elements, as it can tune the relevant parameters, such as electronic density and electron-phonon coupling constants. Recent advances in high-pressure x-ray diffraction techniques have led to the discovery of complex incommensurate crystal structures in the compressed states of elements [7], and these present an unexplored area for searching for a CDW state.

The group VI element sulfur exhibits an incommensurately modulated phase (S-IV) in its metallic state at 300 K and pressures between 83 and 153 GPa [8,9], where atoms are displaced from their ideal positions according to a modulation wave [Fig. 1(a)]. The modulated structure can be described as a distortion of a primitive rhombohedral structure of the β-Po type [Fig. 1(b)], which is found in sulfur at pressures above 153 GPa (phase S-V) at 300 K [8,10]. The transition between the modulated and β-Po phases at 300 K, and the existence of superconductivity at temperatures below 20 K in both phases [11,12], raise the question of whether the occurrence of the incommensurate modulation in sulfur is due to a CDW instability and how this correlates with the superconducting state at low temperatures. If the CDW nature of the modulation is confirmed, sulfur would represent a unique example of an elemental metal undergoing a CDW transition within a superconducting state, and would join a large group of complex materials showing an enhancement of T_c upon pressure-induced suppression of a CDW [3].

Evidence for a CDW transition would include the appearance of a new periodic modulation, the occurrence, in the undistorted phase, of a soft phonon mode with frequency vanishing at the transition, and the presence of a

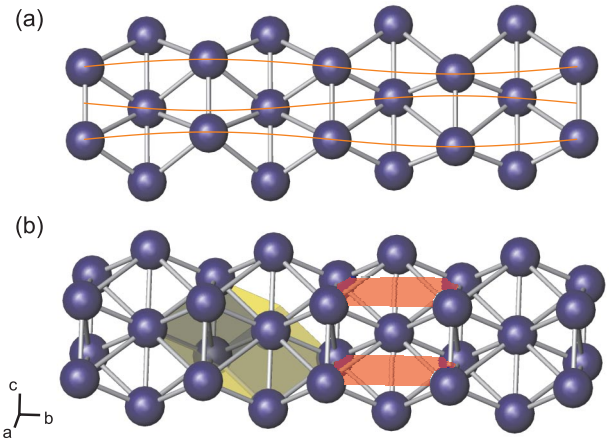

FIG. 1 (color online). Crystal structure of the high-pressure phases of sulfur, (a) S-IV (commensurate approximant is shown) and (b) S-V. Solid lines show the atomic displacement modulation wave with a wave vector of length 1.35 Å^{-1} along the [010] direction (in the bcm setting), which corresponds to a commensurate structure with $q = \frac{3}{4} \times \frac{2\pi}{b}$, used in the calculations. The faces of the primitive rhombohedral β-Po and bcm unit cells are outlined in gray on the left (yellow online) and on the right (red online), respectively, in (b). Crystallographic axes are given for the bcm cell. Interatomic distances up to 2.5 Å are shown.

pronounced "nesting" between parallel regions of the Fermi surface, indicating the electronic character of the transition. Here, using x-ray diffraction, we have measured the amplitude of the atomic displacements in the modulated phase of sulfur at low temperatures close to the superconducting transition. This experimental study is complemented by first-principles calculations of phonon modes, Fermi surfaces, and nesting factors, which show the CDW nature of the transition and provide insight into the correlation between the CDW and superconductivity.

First-principle calculations were performed within density-functional perturbation theory [13] with the QUANTUM-ESPRESSO code [14], using the Perdew-Burke-Ernzerhof [15] generalized gradient approximation for the exchange correlation term. An ultrasoft pseudopotential with an energy cutoff of 35 Ry was used. A uniform $16 \times 16 \times 16$ k-points grid was used to converge phonon frequencies, while a $35 \times 35 \times 35$ grid was used for the calculation of the electron-phonon line width. For the x-ray diffraction measurements, sulfur of 99.9995% purity was loaded together with helium as a pressure transmitting medium into the sample chamber of a rhenium gasket in a membrane driven diamond anvil cell. Powder diffraction data were collected on station ID09a at the European Synchrotron Radiation Facility (ESRF), Grenoble, using an incident x-ray wavelength of 0.4142 Å and an image-plate detector. An online cryostat, cooled by liquid He, was used to achieve sample temperatures down to 15 K. To determine the pressure, we used *in situ* fluorescence measurements of $SrB_4O_7:Sm^{2+}$ with the calibration from Ref. [16]. The temperatures were measured to within ± 5 K by two Si diodes placed next to the sample chamber and on the body of the cell. Rietveld refinement of the integrated diffraction profiles was performed using the JANA2000 software package [17].

Phonon dispersion curves calculated for the β-Po phase of sulfur show a considerable softening of one of the transverse acoustic branches [Fig. 2(a)] along the direction of the distortion in the modulated body-centered monoclinic (bcm) phase ([010]). Calculation of the phonon dispersion along a number of high-symmetry lines in the Brillouin zone of the β-Po structure (Fig. S1 in Ref. [18]) shows that the instability is present only along [010]. The softening becomes less pronounced with pressure and vanishes at 135 GPa with an incommensurate wave vector of length of 1.38 $Å^{-1}$ (Ref. [19]), close to the experimentally obtained value of 1.365(1) $Å^{-1}$ measured at 126 GPa. The electronic Fermi surface (FS) of the unmodulated bcm phase appears to have extended portions connected by the modulation wave vector [Fig. 3(a)] (see also Fig. S2 in Ref. [18]). This, together with the observation of the phonon softening at the modulation wave vector, indicates a CDW origin of the structural modulation [2]. A quantitative assessment of the total extension of the "nested" portions in 3 dimensions (3D) can be obtained by calculating the generalized electronic susceptibility [20]. This has a maximum at the soft mode wave vector [Fig. 3(b)], showing the fundamental role played by FS nesting in the appearance of the CDW.

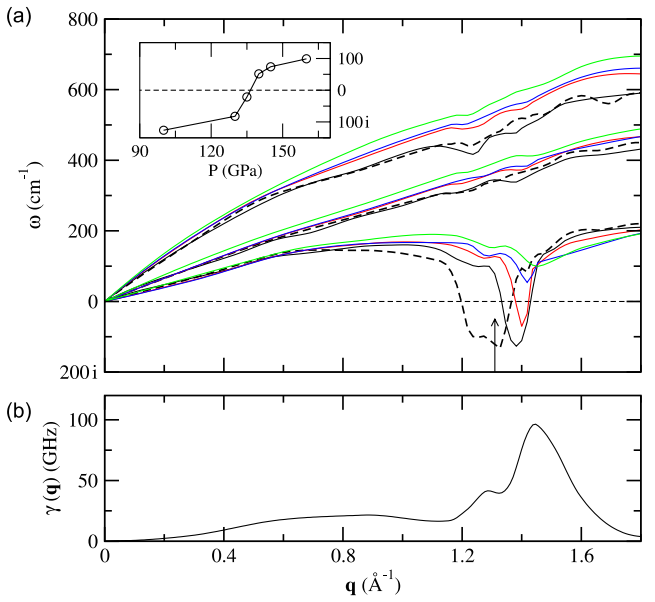

FIG. 2 (color online). (a) Phonon dispersion curves for the β-Po phase at different pressures [medium gray (green online): 160 GPa; dark gray (blue online): 140 GPa; light gray (red online): 130 GPa; black: 100 GPa]. The phonons are calculated along the direction parallel to the [010] direction of the bcm cell. Dashed lines represent the phonon dispersions calculated for the unmodulated bcm structure with the experimental lattice parameters measured at 102 GPa. The arrow shows the value of the modulation vector q, measured at the same pressure. The inset shows the location of the soft mode minimum with pressure in cm^{-1} (calculated for the β-Po phase). (b) Electron-phonon line width along the same [010] direction, for the β-Po phase at 140 GPa.

In order to describe the modulated bcm phase within the periodic-boundary constraint, we constructed a supercell by replicating the 2-atom bcm cell 4 times in the [010] direction, which corresponds to a commensurate modulation with a wave vector $q = 1.35$ $Å^{-1}$ at 100 GPa. Full relaxation of the atomic positions and lattice parameters of this cell leads to the modulated structure shown in Fig. 1(a). The stabilized modulation wave corresponds to an optical phonon where the atoms at the corners and the centers of the monoclinic cell are out of phase. The relaxed structural parameters are consistent with those measured for the S-IV modulated bcm phase (Table S1 in Ref. [18]). Using this commensurate approximant, we calculated the electronic band structure of the modulated bcm structure [Fig. 3(d)], comparing it with that of the unmodulated structure (Fig. S3 in Ref. [18]). The opening of an energy gap along the ΓZ direction ([010]) [Figs. 3(c) and 3(d)] results in a lowering of the electronic density of states at the Fermi level which stabilizes the 1D CDW state. The

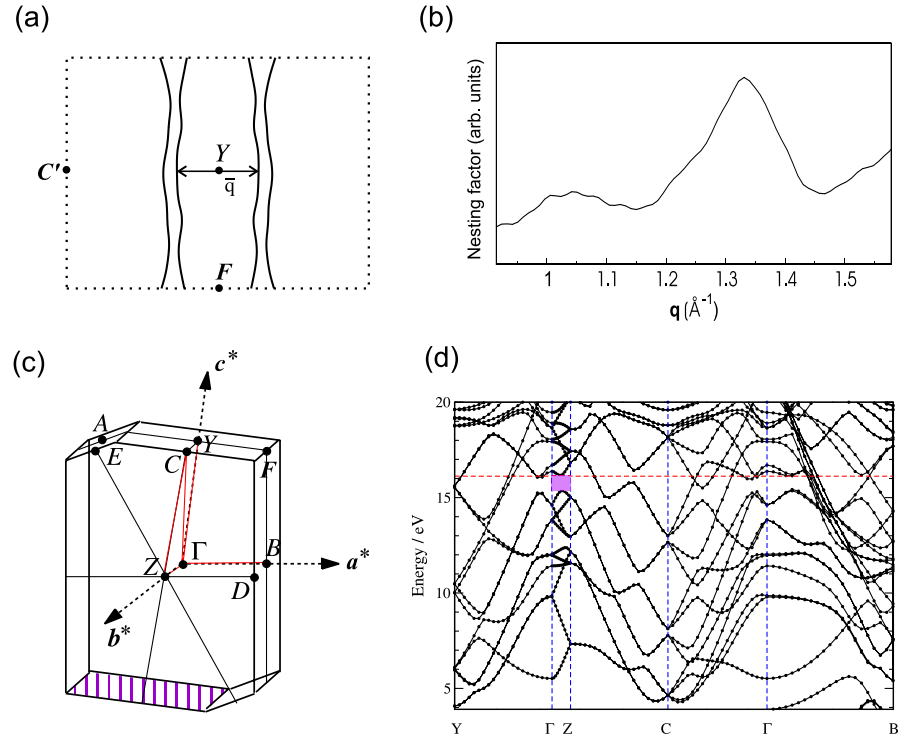

FIG. 3 (color online). (a) Fermi surface cross section (solid lines) calculated for the unmodulated (2-atom) bcm cell at 100 GPa along the CYF plane [dashed plane in (c)]. The Brillouin zone boundary is represented by dotted lines, where the C′Y vector is 4 times longer than the CY vector in (c). The arrow indicates the nesting in the ΓZ ([010]) direction. (b) Generalized susceptibility calculated as a function of q along the [010] direction of the bcm cell (calculated for the unmodulated bcm cell). (c) Brillouin zone for the commensurate approximant containing four bcm cells stacked along [010] (as in Fig. 1). Symmetry points are indicated. (d) Electronic band structure of the modulated bcm structure, calculated for the commensurate approximant, following the path indicated by the light gray (red online) lines in (c). The shaded area highlights a gap that opens in the ΓZ direction due to the modulation.

band structure in the other two perpendicular directions remains metallic and contributes to the residual finite density of states at the Fermi energy (Fig. S4 in Ref. [18]).

Using x-ray diffraction, we observed sharp modulation reflections in S-IV, characteristic of a long-range ordered CDW, and traced their position and intensity as a function of pressure and temperature. From Rietveld refinement of diffraction patterns (Fig. S5 in Ref. [18]) at each P-T point we determined the atomic displacements in S-IV and S-V in the pressure range from 100 to 165 GPa and temperature range from 300 down to 15 K. Within the studied range, the maximum displacement of atoms from their ideal positions of 0.22 Å is found at 100 GPa and 300 K (Fig. 4). This did not change on lowering the temperature down to 15 K at 100 GPa, just a few degrees above the reported T_c [11]. Pressure, however, had a dramatic effect on the amplitude of atomic displacement, which decreased significantly with pressure increase (Fig. 4). The modulation reflections disappear at 140(5) GPa and the structure becomes β-Po at 153(5) GPa [8], signalling the suppression of the CDW.

The pressure dependence of the structural distortion due to the CDW is accompanied by noticeable changes in the behavior of T_c (Fig. 4). Sulfur, a superconductor at pressures above 93 GPa [11], shows a gradual increase of T_c from 10 K to about 14 K on pressure increase within the S-IV phase. The suppression of the CDW at around 150 GPa, as determined from x-ray diffraction, coincides with the observed jump in T_c from 14 to 17 K measured at 155 GPa, the slight difference in pressure possibly arising from the quasihydrostatic (present work) versus nonhydrostatic [11,12] conditions in the experiments. Thus, the present results connect the pressure-induced enhancement of T_c with the suppression of the CDW.

To emphasize the role of the soft mode in the competition between the CDW and superconductivity, we calculated the mode-resolved contribution $\gamma_\nu(q)$ to the electron-phonon line width [21]. The electron-phonon coupling is

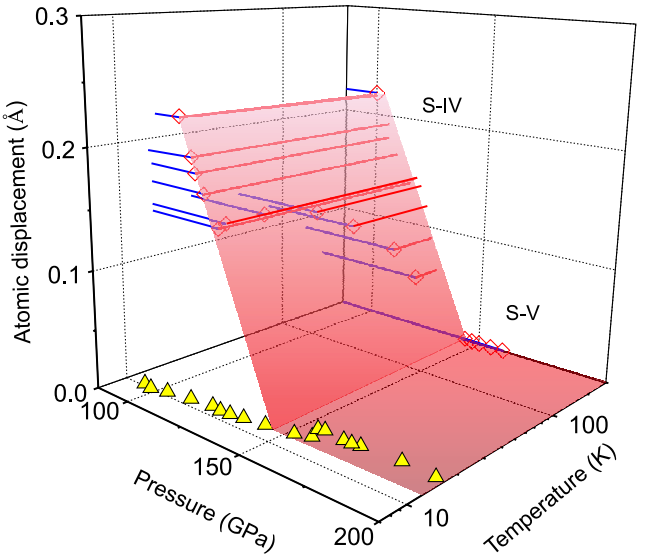

FIG. 4 (color online). Observed maximum atomic displacement in S-IV and S-V as a function of pressure and temperature, shown as open diamond symbols. Lines show different projections of the data. The temperature of the superconducting transition T_c from Ref. [12] is shown by light gray (yellow online) triangles. The temperature is given on a logarithmic scale.

responsible both for the phonon frequency shift which leads to the CDW and for the superconducting transition [22]. The behavior of $\gamma_\nu(q)$ relative to the soft mode, along the direction of the instability, calculated for the β-Po phase in the vicinity of the transition to the CDW state (140 GPa), exhibits a clear peak at the incommensurate wave vector [Fig. 2(b)], which establishes the electron-phonon coupling as the main mechanism driving the phonon instability. The presence of a peak in the $\gamma_\nu(q)$ for the undistorted phase indicates [23] a large contribution of the soft mode to the T_c in the β-Po phase. The transition to the CDW state removes this contribution and opens a gap in the electronic spectrum at the incommensurate wave vector, hence reducing the value of T_c. This explains the reported enhancement of T_c at the transition from the CDW to the undistorted β-Po phase. This behavior is similar to the pressure dependence of T_c observed in Nb chalcogenides and to the doping induced superconductivity reported recently in Cu_xTiSe_2 [3,24].

The incommensurately modulated phases of heavier group VI elements Se and Te [25], isostructural to S-IV, as well as similar phases observed in iodine [26], bromine [27], and phosphorus [28] possibly also exhibit a CDW state. While S, Se, and Te show similar modulations, the behavior of T_c in these elements is different. An explanation for these differences has been proposed for the β-Po phases of S and Se [29]; however, further studies are required to investigate whether this can be extended to the modulated phases.

The authors thank P. Ballone (QUB) for valuable discussions. M. V. M. acknowledges the hospitality of QUB. J. K. and M. V. M. thank the Royal Society for financial support. O. D., M. I. M., and E. G. thank the School of Physics of the University of Edinburgh for material support. Part of the calculations were carried out using the facilities provided by the HPCx consortium, UK. This work is supported by grants from EPSRC, RAS, RFBR, and the facilities provided by the European Synchrotron Radiation Facility.

[1] *Charge Density Waves in Solids*, edited by L. P. Gor'kov and G. Grüner (North-Holland, Amsterdam, 1989).
[2] *Density Waves in Solids*, edited by G. Grüner (Addison-Wesley, Reading, 1994).
[3] A. M. Gabovich, A. I. Voitenko, J. F. Annett, and M. Ausloos, Supercond. Sci. Technol. **14**, R1 (2001).
[4] A. W. Overhauser, Phys. Rev. B **3**, 3173 (1971).
[5] H. G. Smith *et al.*, Phys. Rev. Lett. **44**, 1612 (1980).
[6] L. Fast *et al.*, Phys. Rev. Lett. **81**, 2978 (1998).
[7] M. I. McMahon and R. J. Nelmes, Chem. Soc. Rev. **35**, 943 (2006).
[8] O. Degtyareva, E. Gregoryanz, M. Somayazulu, H. K. Mao, and R. J. Hemley, Phys. Rev. B **71**, 214104 (2005).
[9] C. Hejny, L. F. Lundegaard, S. Falconi, M. I. McMahon, and M. Hanfland, Phys. Rev. B **71**, 020101(R) (2005).
[10] H. Luo, R. G. Greene, and A. L. Ruoff, Phys. Rev. Lett. **71**, 2943 (1993)
[11] V. V. Struzhkin, R. J. Hemley, H. K. Mao, and Y. A. Timofeev, Nature (London) **390**, 382 (1997).
[12] E. Gregoryanz *et al.*, Phys. Rev. B **65**, 064504 (2002).
[13] S. Baroni, S. de Gironcoli, A. Dal Corso, and P. Giannozzi, Rev. Mod. Phys. **73**, 515 (2001).
[14] The QUANTUM-ESPRESSO code is available at http://www.quantum-espresso.org.
[15] J. P. Perdew, K. Burke, and M. Ernzerhof, Phys. Rev. Lett. **77**, 3865 (1996).
[16] F. Datchi, R. LeToullec, and P. Loubeyre, J. Appl. Phys. **81**, 3333 (1997).
[17] V. Petricek, M. Dusek, and L. Palatinus, *JANA2000. The Crystallographic Computing System* (Institute of Physics, Praha, Czech Republic, 2000).
[18] See EPAPS Document No. E-PRLTAO-99-072738 for supplementary materials: figures and a table. For more information on EPAPS, see http://www.aip.org/pubservs/epaps.html.
[19] The given values of q can be related to those in Refs. [8,9] as $1 - \frac{1}{2\pi} qb$.
[20] S. K. Shinain, *Dynamical Properties of Solids*, edited by G. K. Horton and A. A. Maradudin (North-Holland, Amsterdam, 1979), Vol. III.
[21] The mode-resolved electron-phonon line width $\gamma_\nu(q)$ is defined as

$$\gamma_\nu(q) = 2\pi\omega_{q\nu}\sum_k |M^\nu_{k+q,k}|^2 \delta(\varepsilon_k)\delta(\varepsilon_{k+q})$$

where $|M^\nu_{k+q,k}|$ is the electron-phonon matrix element; $\omega_{q,\nu}$ is the phonon frequency at wave vector q and phonon mode index ν; ε_k are the electron eigenvalues; and the sum runs over the Brillouin zone.
[22] P. B. Allen and M. L. Cohen, Phys. Rev. Lett. **29**, 1593 (1972).
[23] G. Profeta *et al.*, Phys. Rev. Lett. **96**, 047003 (2006).
[24] E. Morosan *et al.*, Nature Phys. **2**, 544 (2006).
[25] C. Hejny and M. I. McMahon, Phys. Rev. Lett. **91**, 215502 (2003).
[26] K. Takemura, S. Kyoko, F. Hiroshi, and M. Onoda, Nature (London) **423**, 971 (2003).
[27] T. Kume, T. Hiraoka, Y. Ohya, S. Sasaki, and H. Shimizu, Phys. Rev. Lett. **94**, 065506 (2005).
[28] H. Fujihisa *et al.*, Phys. Rev. Lett. **98**, 175501 (2007).
[29] S. P. Rudin, A. Y. Liu, J. K. Freericks, and A. Quandt, Phys. Rev. B **63**, 224107 (2001).